Heliyon

CrossMark

Hydrogen peroxide induced cell death: One or two modes of action?

Lionel Uhl, Audrey Gerstel, Maialène Chabalier, Sam Dukan [*]

Institut de Microbiologie de la Méditerranée – Université Aix-Marseille, Laboratoire de Chimie Bactérienne, CNRS UMR7283, 31 Chemin Joseph Aiguier, 13009 Marseille, France

[*] Corresponding author at: Aix-Marseille Université, Laboratoire de Chimie Bactérienne (UMR7283), Institut de Microbiologie de la Méditerranée (IMM), CNRS, 31 Chemin Joseph Aiguier, 13402 Marseille, France. Fax: +33 4 91 71 89 14; tel.: +33 4 91 16 46 01.
E-mail address: sdukan@imm.cnrs.fr (S. Dukan).

Abstract

Imlay and Linn show that exposure of logarithmically growing *Escherichia coli* to hydrogen peroxide (H_2O_2) leads to two kinetically distinguishable modes of cell killing. Mode one killing is pronounced near 1 mM concentration of H_2O_2 and is caused by DNA damage, whereas mode-two killing requires higher concentration (> 10 mM). The second mode seems to be essentially due to damage to all macromolecules. This phenomenon has also been observed in Fenton *in vitro* systems with DNA nicking caused by hydroxyl radical ($HO^\bullet$).

To our knowledge, there is currently no mathematical model for predicting mode one killing *in vitro* or *in vivo* after H_2O_2 exposure.

We propose a simple model, using *Escherichia coli* as a model organism and a set of ordinary differential equations. Using this model, we show that available iron and cell density, two factors potentially involved in ROS dynamics, play a major role in the prediction of the experimental results obtained by our team and in previous studies. Indeed the presence of the mode one killing is strongly related to those two parameters.

To our knowledge, mode-one death has not previously been explained. Imlay and Linn (Imlay and Linn, 1986) suggested that perhaps the amount of the toxic species was reduced at high concentrations of H_2O_2 because hydroxyl (or other) radicals might be quenched directly by hydrogen peroxide with the concomitant formation

of superoxide anion (a less toxic species). We demonstrate (mathematically and numerically) that free available iron decrease is necessary to explain mode one killing which cannot appear without it and that H_2O_2 quenching or consumption is not responsible for mode-one death.

We are able to follow ROS concentration (particularly responsible for mode one killing) after exposure to H_2O_2. This model therefore allows us to understand two major parameters involved in the presence or not of the first killing mode.

Keywords: Mathematical biosciences, Mathematical modelling, Systems biology

1. Introduction

The principal reactive oxygen species (ROS) — superoxide $O_2^{\bullet-}$, hydrogen peroxide H_2O_2, and the hydroxyl radical $HO^\bullet$ — are generated by sequential reductions of molecular oxygen and are continually produced in cells. Oxidative stress results from an imbalance between exposure to ROS and defenses against ROS, potentially causing damage to all macromolecules (Imlay, 2013). There is increasing evidence to suggest that the cumulative damage caused by ROS contributes to many diseases, including age-related disorders, such as Parkinson's disease and Alzheimer's disease, and cancer (Jimenez-Del-Rio and Velez-Pardo, 2012).

The ability of bacteria to cope with these ROS species has been studied in detail (Fridovich, 1978; Keyer and Imlay, 1996; Park et al., 2005; Kowald et al., 2006; Gonzalez-Flecha and Demple, 1995; Seaver and Imlay, 2004; Hillar et al., 2000; Aslund et al., 1999). Briefly, in *Escherichia coli*, cytoplasmic superoxide dismutases (Mn-SOD and Fe-SOD) constitute the principal system responsible for keeping $O_2^{\bullet-}$ concentration below 2×10^{-10} M (Imlay and Fridovich, 1991). Alkyl hydroperoxide reductase (Ahp) and catalases (KatG and KatE) keep H_2O_2 concentration below 20 nM (Seaver and Imlay, 2001b). These concentrations of these two ROS species need to be kept very low as they are linked to the formation of $HO^\bullet$ via the Fenton reaction ($H_2O_2 + Fe^{2+} \rightarrow HO^\bullet + HO^- + Fe^{3+}$), against which cells have no known defense (Imlay et al., 1988). Indeed, $O_2^{\bullet-}$ rapidly destroys the [4Fe–4S] clusters of dehydratases, leading to the release of reactive iron (Fe^{2+}), which may then react with H_2O_2 to generate $HO^\bullet$ (Fenton reaction).

Imlay and Linn (Imlay and Linn, 1986; Imlay et al., 1988) show that exposure of logarithmically growing *E. coli* to H_2O_2 involves two kinetically modes of cell killing. Mode one killing pronounced near 1 mM concentration of H_2O_2 is caused

by DNA damage, whereas mode-two killing appears with higher concentration (> 10 mM) and seems to be essentially due to damage to all macromolecules.

In this study, we aimed to use *E. coli* as a model organism, to investigate *ROS* dynamics and to understand the presence or not of the first killing mode. We used data from a large number of articles dealing with enzyme or molecule concentrations, kinetic properties and chemical reaction rate constants to generate a mathematical model based on a set of ordinary differential equations relating to fundamental principles of mass balance and reaction kinetics. To our knowledge, no such mathematical model allowing the prediction of ROS concentration and explanation of mode one killing, after H_2O_2 exposure, has ever been developed before.

2. Materials and methods

All numerical simulations were carried out using the MATLAB ODE solver ode15s for stiff differential equations. The multistep solver ode15s is a variable order solver based on the numerical differentiation formulas.

3. Results and discussion

3.1. The key role of free iron, its decrease during oxidative stress

The first aim of this study was to determine whether *in vivo* Fe^{2+} should be taken into account as variable when trying to predict the mode one killing. Our interest in Fe^{2+} stems from its involvement in the Fenton reaction, which leads to the formation of $HO^\bullet$. It is therefore important to determine whether Fe^{2+} concentration can be assumed to be constant, as a first approximation, or whether it must be treated as variable, when estimating $HO^\bullet$ concentration. Indeed, literature shows studies considering free iron as a constant (Antunes et al., 1996) and other presenting iron evolution (Bertrand, 2014).

Our study will not mention copper. Indeed although either copper or iron can reduce H_2O_2 *in vitro*, iron is the responsible species *in vivo*. Indeed, the amount of available copper may be too small. Imlay indicates that mutants that lose the ability to control copper levels exhibit normal resistance to H_2O_2 (Macomber et al., 2007). Thus, copper is liganded by the large pool of intracellular thiols (including glutathione which is in millimolar concentration) that blocks the participation of copper in $HO^\bullet$ formation *in vitro*. Moreover, H_2O_2-oxidizable copper is located in the periplasm; therefore, most of the copper-mediated hydroxyl radical formation occurs in a compartment far away from DNA.
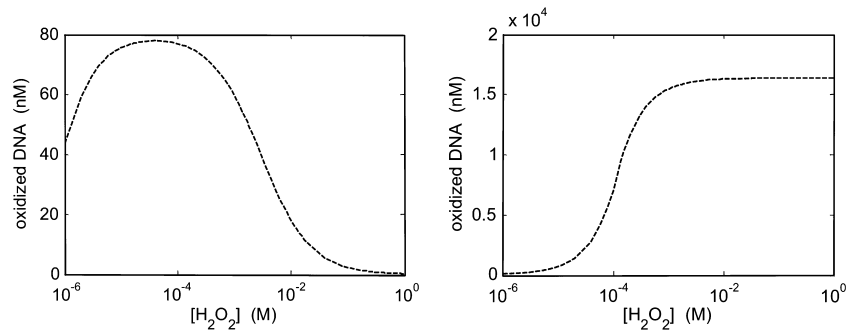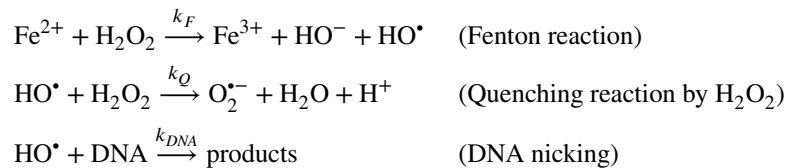
Figure 1. Simulation for H_2O_2-mediated mode 1 killing (left panel) in a Fenton system obtained with 80 nM of Fe^{2+} and 17 μM DNA. Mode one killing disappear (right panel) when free iron is artificially taken constant (the dynamical system has been modified by taken $d\left[Fe^{2+}\right]/dt = 0$).

3.1.1. A simple in vitro system

The simplest *in vitro* system was proposed by Luo et al. (1994) only considering 80 nM of Fe^{2+} and 17 μM DNA. They show that DNA nicking is maximal at 0.05 mM H_2O_2 concentration after a 7.5 minutes experiment.

The chemical reactions which describe this system are:

$$Fe^{2+} + H_2O_2 \xrightarrow{k_F} Fe^{3+} + HO^- + HO^\bullet \quad \text{(Fenton reaction)}$$

$$HO^\bullet + H_2O_2 \xrightarrow{k_Q} O_2^{\bullet-} + H_2O + H^+ \quad \text{(Quenching reaction by } H_2O_2)$$

$$HO^\bullet + DNA \xrightarrow{k_{DNA}} products \quad \text{(DNA nicking)}$$

The resulting dynamical system of ordinary differential equation is:

$$\frac{d\left[HO^\bullet\right]}{dt} = k_F\left[Fe^{2+}\right]\left[H_2O_2\right] - k_Q\left[HO^\bullet\right]\left[H_2O_2\right] - k_{DNA}[DNA]\left[HO^\bullet\right]$$

$$\frac{d\left[Fe^{2+}\right]}{dt} = -k_F\left[Fe^{2+}\right]\left[H_2O_2\right]$$

$$\frac{d\left[H_2O_2\right]}{dt} = -k_F\left[Fe^{2+}\right]\left[H_2O_2\right] - k_Q\left[HO^\bullet\right]\left[H_2O_2\right]$$

$$\frac{d[DNA]}{dt} = -k_{DNA}[DNA]\left[HO^\bullet\right]$$

Taking the reaction rate constants found in literature, $k_F = 4.4 \times 10^4$ M s^{-1} (Park et al., 2005), $k_Q = 2.7 \times 10^7$ M s^{-1} (Buxton and Greenstock, 1988) and $k_{DNA} = 4.7 \times 10^9$ M s^{-1} (Michaels and Hunt, 1973), the simulation shows exactly the same maximum (Fig. 1) when reporting average DNA nicking (during time experiment) versus H_2O_2 concentration.

In this system, it is obvious that free iron decreases because there is no way of recycling; nevertheless we present a hypothetic simulation considering free iron as

a constant. This hypothetic simulation realized with $d\left[\text{Fe}^{2+}\right]/dt = 0$ makes clear the need to take into account free iron as a variable even in a simple system in order to see mode one killing; and it also shows that iron decrease is responsible of the first killing mode. Imlay first discussion (Imlay and Linn, 1986) concerning the quenching of HO$^{\bullet}$ with H_2O_2 in order to interpret mode one killing have to be forgotten. The quenching only slows down the DNA oxidation (caused by HO$^{\bullet}$) but it cannot be responsible for the mode one killing.

3.2. Mathematical analysis of the *in vivo* Fenton system

DNA nicking involves a reaction between DNA and HO$^{\bullet}$, therefore, in order to see mode one killing, HO$^{\bullet}$ concentration must reach a maximum as a function of exogenous H_2O_2 concentration. Considering *in vivo* Fenton system we have to take into account H_2O_2 scavenging enzyme (Alkyl hydroperoxide reductase and catalases). Let us examine whether this system is consistent with a maximum level of HO$^{\bullet}$ concentration when challenging H_2O_2. Our model does not take into account molecules compartmentalization (see justification in Supplementary Material B).

HO$^{\bullet}$ depends on time t and $\left[\text{H}_2\text{O}_2\right]_{out}$ (exogenous H_2O_2 concentration). If HO$^{\bullet}$ reaches a maximum value, that implies that a mathematical derivative of HO$^{\bullet}$ versus $\left[\text{H}_2\text{O}_2\right]_{out}$ reached zero. Before evaluating $\frac{d\left[\text{HO}^{\bullet}\right]}{d\left[\text{H}_2\text{O}_2\right]_{out}}$, we need to know how HO$^{\bullet}$ levels change.
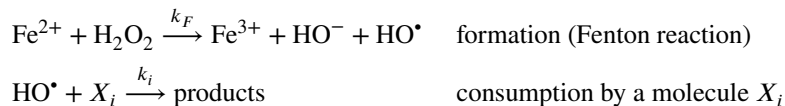
The most important cellular sinks for hydroxyl radical are reactions with major cellular components like proteins, metabolomes, … The quenching reaction (with H_2O_2) may be relevant under *in vitro* conditions when H_2O_2 concentration is very high (and DNA concentration very low), but under a physiological setting or even when cells are exposed to external H_2O_2, H_2O_2 will not be a major sink for hydroxyl radical. Indeed, reaction rate constant of HO$^{\bullet}$ between organic cellular compounds (like proteins, metabolomes, …) are closed to diffusion limit rate constant $k_{diff} \approx 10^{10}\ \text{M}^{-1}\ \text{s}^{-1}$ and organic cellular compounds concentration $\left[Organic\right]$ is higher than 10 mM, therefore under the mode one killing where H_2O_2 concentration is under 4 mM, we can write the inequality:

$$\frac{v_{organic\ sinks}}{v_{quenching}} = \frac{k_{diff}\left[Organic\right]\left[\text{HO}^{\bullet}\right]}{k_Q\left[\text{H}_2\text{O}_2\right]\left[\text{HO}^{\bullet}\right]} = \frac{k_{diff}\left[Organic\right]}{k_Q\left[\text{H}_2\text{O}_2\right]} \approx 10^3 \gg 1$$

This inequality means that the quenching reaction can be neglected in the study of mode one killing.

Moreover, concerning HO$^{\bullet}$ production, we do not consider Haber–Weiss reaction, a reaction whose relevance *in vivo* is questionable

([Koppenol, 2001; Liochev and Fridovich, 2002](#)). In fact, when adding this reaction, we saw no significant change in ROS or DNA kinetic. Therefore, within cells, for a given exogenous H_2O_2 concentration, $HO^\bullet$ levels obey the following reactions:

$$Fe^{2+} + H_2O_2 \xrightarrow{k_F} Fe^{3+} + HO^- + HO^\bullet \quad \text{formation (Fenton reaction)}$$

$$HO^\bullet + X_i \xrightarrow{k_i} \text{products} \qquad\qquad \text{consumption by a molecule } X_i$$

In vivo, because $HO^\bullet$ reacts with various molecules we generalise the system and demonstrate that we need to consider available iron as a variable.

Proof by contradiction (*reductio ad absurbum*): Suppose that free iron is constant.

Considering N reactions (of rate constant k_i between an organic X_i compound and $HO^\bullet$) and assuming X_i concentration is constant because X_i is in large excess (for example DNA, proteins, metabolomes, . . .). Therefore $HO^\bullet$ levels obey the following kinetic differential equation:

$$\frac{d\left[HO^\bullet\right]}{dt} = k_F\left[Fe^{2+}\right]\left[H_2O_2\right] - \sum_{i=1}^{N} k_i\left[HO^\bullet\right]\left[X_i\right]$$

The resolution of this equation gives:

$$\left[HO^\bullet\right] = \left(\int_0^t k_F\left[Fe^{2+}\right]\left[H_2O_2\right]\exp\left(\sum_{i=1}^{N} k_i\left[X_i\right]t'\right)dt'\right)\exp\left(-\sum_{i=1}^{N} k_i\left[X_i\right]t\right)$$

$$(*)$$

Internal H_2O_2 concentration is also dependent on t and $\left[H_2O_2\right]_{out}$, as follows:

$$\left[H_2O_2\right] = f\left(t, \left[H_2O_2\right]_{out}\right)$$

In addition, the more exogenous H_2O_2 added, the more H_2O_2 penetrates the cell, so f is a monotonic increasing function of $\left[H_2O_2\right]_{out}$ and $\frac{\partial f\left(\left[H_2O_2\right]_{out}, t\right)}{\partial\left[H_2O_2\right]_{out}} > 0$. The mathematical derivative of $HO^\bullet$ versus $\left[H_2O_2\right]_{out}$ gives:

$$\frac{d\left[HO^\bullet\right]}{d\left[H_2O_2\right]_{out}} = \left(\int_0^t k_F\left[Fe^{2+}\right]\frac{\partial f\left(\left[H_2O_2\right]_{out}, t'\right)}{\partial\left[H_2O_2\right]_{out}}\exp\left(\sum_{i=1}^{N} k_i\left[X_i\right]t'\right)dt'\right)$$

$$\times \exp\left(-\sum_{i=1}^{N} k_i\left[X_i\right]t\right)$$

This expression obviously indicates that $\frac{d\left[HO^\bullet\right]}{d\left[H_2O_2\right]_{out}} > 0$ because all terms are positive.

For this reason, in this model, there should be no peak when changes in $HO^{\bullet}$ levels are plotted against exogenous H_2O_2 levels. This conclusion is in contradiction with mode one killing observation, therefore we must consider Fe^{2+} concentration to decrease with increasing H_2O_2 concentration.

We can notice that a direct proof, without supposing free iron constant, gives by derivation of (∗):

$$\frac{d\left[HO^{\bullet}\right]}{d\left[H_2O_2\right]_{out}} = \left(\int_0^t k_F F_{(Fe^{2+}, H_2O_2)} \exp\left(\sum_{i=1}^N k_i\left[X_i\right]t'\right)dt'\right)$$

$$\times \exp\left(-\sum_{i=1}^N k_i[X_i]t\right)$$

where $F_{(Fe^{2+},[H_2O_2])} = \left[\left[Fe^{2+}\right]\frac{\partial f\left(\left[H_2O_2\right]_{out}, t'\right)}{\partial\left[H_2O_2\right]_{out}} + \left[H_2O_2\right]\frac{\partial\left[Fe^{2+}\right]}{\partial\left[H_2O_2\right]_{out}}\right]$.

This expression can reach zero only if:

$$\underbrace{\left[Fe^{2+}\right]}_{>0}\underbrace{\frac{\partial f\left(\left[H_2O_2\right]_{out}, t'\right)}{\partial\left[H_2O_2\right]_{out}}}_{>0} + \underbrace{\left[H_2O_2\right]}_{>0}\frac{\partial\left[Fe^{2+}\right]}{\partial\left[H_2O_2\right]_{out}} = 0$$

It demonstrates that necessarily $\frac{\partial\left[Fe^{2+}\right]}{\partial\left[H_2O_2\right]_{out}} < 0$, meaning that $\left[Fe^{2+}\right]$ is a monotonic decreasing function of $\left[H_2O_2\right]_{out}$.

So, to explain the experimental curve for DNA nicking *in vitro*, we must consider Fe^{2+} concentration to decrease with increasing H_2O_2 concentration.

3.2.1. Mathematical model

The first difference between *in vivo* and *in vitro* experiments is the value of H_2O_2 exogenous concentration needed to reach maximum in the mode one killing (Imlay et al., 1988). This difference is for a number of reasons. First cell membrane and cell scavenger (Ahp and catalase) reduce H_2O_2 concentration within the cell; therefore mode one killing appears with higher concentration of H_2O_2 concentration *in vivo*. Then there are many sinks for hydroxyl radical and free iron evolution has to take its recycling into account. The model has to be completed with the following equations, of course we only present the major reaction involved in the description of the mode one killing; for instance we do not add reaction between organic compounds and H_2O_2 which is negligible when compared to enzymatic dismutation. This model is deliberately simple in order to examine the predominant effects.

Internal hydrogen peroxide kinetics

$$\frac{d\left[H_2O_2\right]}{dt} = k_{prod}^{H_2O_2} \qquad\qquad\qquad : \text{Endogenous production}$$

$$-\frac{k_{cat}^{Ahp}\left[Ahp\right]\left[H_2O_2\right]}{\left[H_2O_2\right] + K_M^{Ahp}} \qquad : \text{Dismutation by Ahp } H_2O_2 \xrightarrow{Ahp} H_2O + 1/2O_2$$

$$-\frac{k_{cat}^{Kat}\left[Kat\right]\left[H_2O_2\right]}{\left[H_2O_2\right] + K_M^{Kat}} \qquad : \text{Dismutation by Kat } H_2O_2 \xrightarrow{Kat} H_2O + 1/2O_2$$

$$- k_{diff}\left(\left[H_2O_2\right] - \left[H_2O_2\right]_{ex}\right) \;:\; \text{Diffusion across cell membrane}$$

$$- k_F\left[H_2O_2\right]\left[Fe^{2+}\right] \qquad\quad : \text{Fenton reaction}$$

External hydrogen peroxide concentration ($\left[H_2O_2\right]_{out}$) strongly depends on cell number (noted n), indeed, the higher cell density, the faster the media is detoxified. The cell density involvement will be discussed in section 3.3.

External hydrogen peroxide kinetics

$$\frac{d\left[H_2O_2\right]_{out}}{dt} = k_{diff}\frac{n \cdot V_{internal}}{V_{external}}\left(\left[H_2O_2\right] - \left[H_2O_2\right]_{out}\right)$$

$V_{internal}$ represents intracellular solvent-accessible volume.

Cell numbers n double every 20 minutes according to an exponential law.

Hydroxyl radical kinetics

We consider N reactions of rate constant k_i between an organic X_i compound (proteins, metabolites, …) and $HO^\bullet$. Nevertheless, DNA was treated separately (out of the sum) in order to examine its damage during oxidative stress, so it comes to the following equations:

$$\frac{d\left[HO^\bullet\right]}{dt} = k_F\left[Fe^{2+}\right]\left[H_2O_2\right] - \sum_{i=1}^{N} k_i\left[X_i\right]\left[HO^\bullet\right] - k_{DNA}\left[DNA\right]\left[HO^\bullet\right]$$

$$\frac{d\left[DNA\right]}{dt} = -k_{DNA}\left[DNA\right]\left[HO^\bullet\right]$$

Recycling of free iron

Free available Fe^{2+} is oxidized during Fenton reaction but Fe^{3+} is then reduced by cellular reductants. However, the identity of the biological reductants *in vivo* remains unclear (Valko et al., 2005), Fe^{3+} might also be reduced at varying
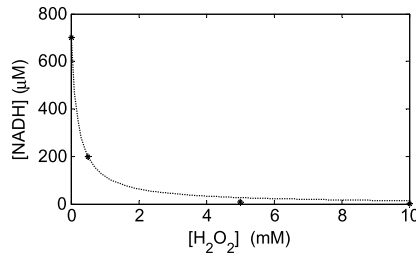
Figure 2. *In vivo* NADH levels after H_2O_2 challenge of *E. coli* (* marker for Brumaghim measurements and dots for our mathematical model).

reaction rates by a range of cellular reductants, such as glutathione, L-cysteine, NAD(P)H and $FADH_2$ (Imlay, 2003). The kinetic of iron recycling has to take into account the fact that reductant concentrations also decrease with increasing value of exogenous concentration of H_2O_2 because of reductant reactions with various ROS. For instance Brumaghim et al. report that *in vivo* NADH concentration reduce by half when challenging about 0.2 mM of H_2O_2 (Fig. 2). Therefore we corrected recycling rate with a Hill factor (noted f) of coefficient 1 (because decrease is hyperbolic) often used to describe reaction of inhibition (Polynikis et al., 2009). We consider here that H_2O_2 inhibits the efficiency of the reductants to recycle Fe^{3+} into Fe^{2+}.

For instance, reduction by NADH gives the kinetic rate:

$$v_{red}^{NADH} = k_{NADH} \left[Fe^{3+} \right] [NADH]$$

where $[NADH] = f_{NADH}[NADH]_0$ and $f_{NADH} = \dfrac{C_{1/2}^{NADH}}{[H_2O_2] + C_{1/2}^{NADH}}$ where $C_{1/2}^{NADH}$ is the H_2O_2 concentration needed to reduce by half the initial concentration of NADH.

$[NADH]_0$ represents NADH concentration without oxidative stress.

Hill correction factor fits Brumaghim experimental results by taking $C_{1/2}^{NADH} = 0.2$ mM (this value was found using a least square approximation).

We can then write Fe^{3+} reduction kinetic rate by NADH:

$$v_{red}^{NADH} = k_{NADH} \left[Fe^{3+} \right] [NADH]_0 \frac{C_{1/2}^{NADH}}{\left[H_2O_2 \right] + C_{1/2}^{NADH}}$$

or

$$v_{red}^{NADH} = k_{NADH}[NADH]_0 [Fe] \frac{[Fe] - \left[Fe^{2+} \right]}{[Fe]} \frac{C_{1/2}^{NADH}}{\left[H_2O_2 \right] + C_{1/2}^{NADH}}$$

because $\left[Fe^{3+} \right] = [Fe] - \left[Fe^{2+} \right]$ where [Fe] represents the total free available iron concentration in cell.

We can also write

$$v_{red}^{NADH} = v_{max}^{NADH} \frac{[Fe] - [Fe^{2+}]}{[Fe]} \frac{C_{1/2}^{NADH}}{[H_2O_2] + C_{1/2}^{NADH}}$$

where $v_{max}^{NADH} = k_{NADH}[NADH]_0 [Fe]$

According to Brumaghim et al. (2003) NADH oxidation experiment, 16 μM of *in vitro* initial NADH concentration are oxidized by 80 μM of Fe^{3+} with an initial rate constant (obtained by measurement of NADH absorbance at 340 nm) $k_{NADH} [Fe^{3+}] = 2.3 \times 10^{-4} \, s^{-1}$, so with physiological concentration, the maximal rate constant for Fe^{3+} reduction will be near $k_{NADH}[NADH]_0 [Fe] = 10^{-7} \, M \, s^{-1}$.

Brumaghim et al. produce the same study with NADPH, and according to their experimental results we have $k_{NADPH}[NADPH]_0 [Fe] = 4 \times 10^{-9} \, M \, s^{-1}$ and $C_{1/2}^{NADPH} = 4$ mM.

Moreover, cell counts many reductants like ascorbate which may represent an alternative way to generate Fe^{2+} (Hsieh and Hsieh, 2000). Thiols and in particular glutathione GSH in physiological systems, are important agents responsible for helping to maintain aerobic cells in a reducing state, despite an oxidizing environment. Nevertheless, a growing body of evidence suggests that thiols, as electron donors of metal-catalyzed oxidation systems, can paradoxically be responsible for the generation of reactive oxygen species (Giannessi et al., 1993). For instance, Netto and Stadtman (1996) report that Dithiothreitol reduces Fe^{3+} with a constant rate near 2.5 $M^{-1} \, s^{-1}$, therefore $v_{max}^{RSH} = k_{RSH} [Fe] [RSH]_0 \geq 10^{-6} \, M \, s^{-1}$.

We can notice that the upper limit for $v_{max}^{Red} = k_{Red} [Fe] [Red]_0$ is near $10^3 \, M \, s^{-1}$ (using the rate constant of diffusion limited reaction which is near $10^{10} \, M^{-1} \, s^{-1}$, and assuming $[Red] \leq 10^{-2}$ M and $[Fe] \approx 20$ μM). Of course the real (but unknown) value should be much weaker.

By adding N reductants (noted R_i), reduction rate can be written:

$$v_{red} = \sum_{i=1}^{N} \left(v_{max,i} \frac{[Fe] - [Fe^{2+}]}{[Fe]} \frac{C_{1/2}^{i}}{[H_2O_2] + C_{1/2}^{i}} \right)$$

Of course, we cannot find the values of all kinetic constants in literature for *in vivo* system whereas it is a crucial issue; we therefore use an average formula with only two constants:

$$v_{red} = v_{max} \frac{C_0}{[H_2O_2] + C_0} \frac{[Fe] - [Fe^{2+}]}{[Fe]}$$

When $[H_2O_2] \rightarrow C_0$, the efficiency of the reduction is reduced by half, v_{max} represents the maximal rate of Fe^{3+} reduction, this rate is obtained in a hypothetic

scheme when $[H_2O_2] \rightarrow 0$ (meaning that reductants are the most efficient at low H_2O_2 concentration) and when $[Fe^{2+}] \rightarrow 0$ (meaning that Fe^{3+} concentration is maximal).

We then have to examine the involvement of these two constants (v_{max} and C_0) on mode one killing. Finally free iron kinetic is approached to:

$$\frac{d[Fe^{2+}]}{dt} = -k_F [Fe^{2+}] [H_2O_2] + v_{max} \frac{C_0}{[H_2O_2] + C_0} \frac{[Fe] - [Fe^{2+}]}{[Fe]}$$

The Fig. 3 represents the principal interactions between the reagents used in the mathematical model.

Scheme of the model
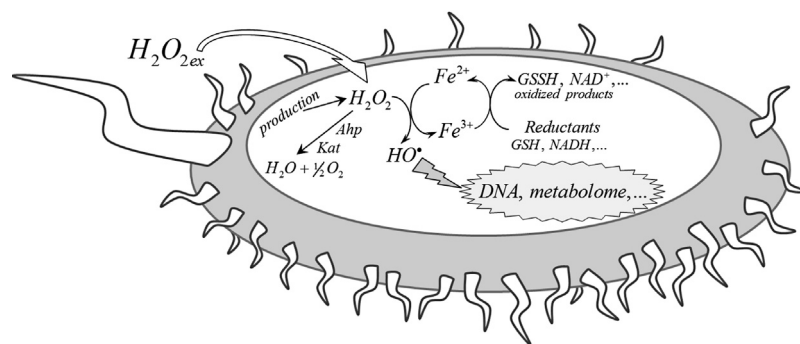
Figure 3. Scheme of ROS interaction in the mathematical model.

3.2.2. Choice of kinetic constants

According to Park et al. (2005) experiments, at 37 °C and neutral pH, the Fenton rate constant for DNA-bound iron was $k_F = 4400\ \mathrm{M\,s^{-1}}$ but this constant is higher when iron is bound to ATP. As mode one killing concerns DNA damage, we use $k_F = 4400\ \mathrm{M\,s^{-1}}$ for our simulation. Indeed HO$^{\bullet}$ reacts very fast and therefore only impacts the nearest organic compounds.

DNA concentration refers to nitrogenous bases concentration, this concentration is set to 5×10^{-3} M, corresponding to approximately 4.6×10^6 pairs (with the proportion of each base set at 25%, which is close to the value proposed by the CBS genome atlas database of Hallin and Ussery (2004)).

We then consider N reactions of rate constant k_i between an organic X_i compound (or site) and HO$^{\bullet}$ ($\sum_{i=1}^{N} k_i [X_i] [HO^{\bullet}]$). For instance Bennett et al. (2009) report total metabolome concentration of 300 mM (100 millions metabolites/cell)

greatly exceeded the reported total protein concentration of 7 mM (2.4 million proteins/cell). Nevertheless, with an average of 400 residues per protein, it represents 2.8 M of feeding sites for $HO^\bullet$.

We assume that $\sum_{i=1}^{N} k_i [X_i] \approx 7.3 \times 109$ s^{-1} (Supplementary Material A), which corresponds to a mean rate constant of 2×109 $M\,s^{-1}$ for reaction between $HO^\bullet$ and organic compounds.

3.2.3. Position and width of mode one killing

Position of mode one killing corresponds to the concentration of H_2O_2 where the maximum of DNA damage occurs. Position and width of mode one killing of course depend on reaction rate constants and in particular on the recycling rate of free iron characterized by v_{max} and C_0. Mode one killing can also be described by its intensity (DNA oxidized proportion) but it is impossible to directly link bacterial survival curve to intensity of DNA oxidized proportion whereas survival bacterial curve should occur at the same position and should present approximately the same shape. Therefore we focus on the position and the width of mode one killing. We previously show the particular importance of iron evolution; therefore we will next focus on the two parameters v_{max} and C_0 introduced to describe its kinetic.

The influence of v_{max}

For next simulations we set $C_0 = 1$ mM (the influence of this constant will be discussed later) and we observe the influence of the parameter v_{max}. According to the previous discussion $v_{max} > 10^{-6}$ $M\,s^{-1}$.

Fig. 4 shows that an increasing value of v_{max} involves a higher position of mode-one killing but also a higher intensity of DNA oxidation. Indeed v_{max} is linked to the cell potential to reduce Fe^{3+} to Fe^{2+} and therefore to drive Fenton reaction more efficiently.

The simulations are consistent with the mode-one killing experimental position near 1–3 mM.

When Fe^{2+} recycling rate is too high (inset Fig. 4) mode-one killing disappear because Fe^{2+} concentration remains constant.

Moreover, Imlay et al., (Imlay et al., 1988) showed that if the availability of cellular reducing equivalents is increased as the result of respiration inhibition (through cyanide and NADH dehydrogenase mutations), mode I killing was enhanced. Our model is able to reproduce this phenomenology, as demonstrated by
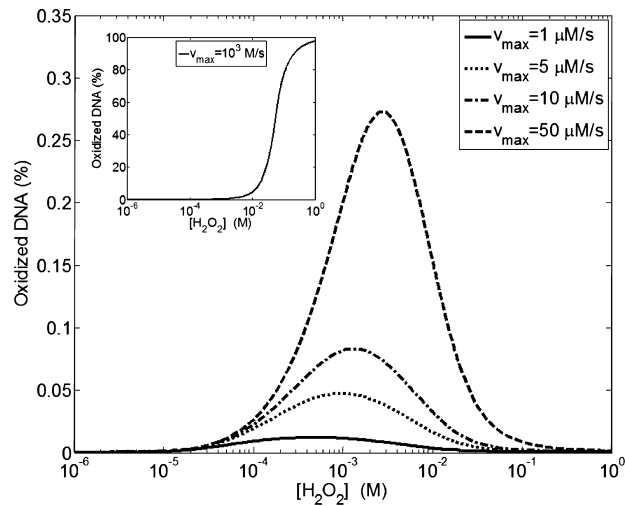
Figure 4. Average DNA oxidation (during 15 minutes) dependence upon H_2O_2 external concentration and maximal Fe^{2+} recycling rate v_{max}. C_0 is set to 1 mM. Initially, cell density was set to 10^7 cell/mL. The kinetic parameters used for the simulation are gathered in Table 1.

Table 1. Summary of the different constants used for *in silico* simulations.

Constants	Value	Reference
$k_{prod}^{H_2O_2}$	$15\ \mu M\,s^{-1}$	Seaver and Imlay, 2001a, 2004
K_M^{Kat}	5.9×10^{-3} M	Hillar et al., 2000
K_M^{Ahp}	1.2×10^{-6} M	Seaver and Imlay, 2001b
k_{cat}^{Kat} [Kat]	$4.9 \times 10^{-1}\ M\,s^{-1}$	,,
k_{cat}^{Ahp} [Ahp]	$6.6 \times 10^{-4}\ M\,s^{-1}$	,,
k_{diff}	$70\ s^{-1}$	,,
$V_{internal}$	3.2×10^{-15} L	Imlay and Fridovich, 1991
k_{DNA}	$4.7 \times 10^9\ M\,s^{-1\,*}$	Michaels and Hunt, 1973
k_F	$4400\ M\,s^{-1}$	Park et al., 2005
Initial Fe^{2+} concentration	By default $20\ \mu M^{**}$	,,
Initial cell density n	From 10^6 to 10^9	
C_0	Tested from 0.1 to 5 mM	This work
v_{max}	Tested from 1 to $50\ \mu M\,s^{-1}$ and $3\ M\,s^{-1}$	This work
Simulation time	15 minutes	Imlay and Linn, 1986, 1988

* This value is limited the *in vivo* diffusion-limited rate constant assumed to be $2 \times 10^9\ M\,s^{-1}$ (Supplementary Material A).

** We also tested value from 10 to 40 μM for the simulation showed in Fig. 6.

the direct correlation between the v_{max} parameter and the percentage of oxidized DNA (Fig. 4).
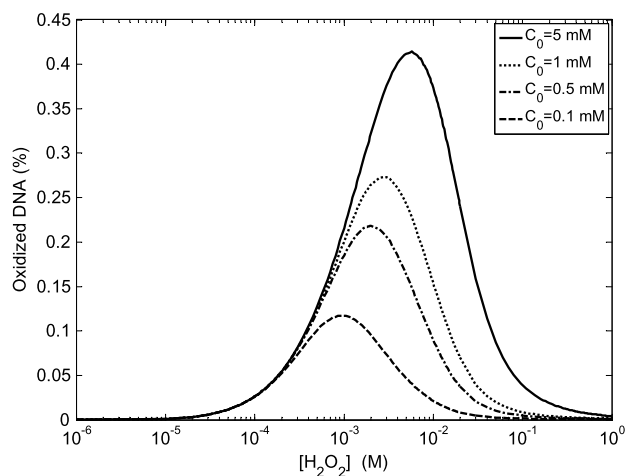
Figure 5. Average DNA oxidation (during 15 minutes) dependence upon H_2O_2 external concentration and parameter C_0. v_{max} is set to 50 µM s^{-1}. Initially, cell density was set to 10^7 cell/mL. The kinetic parameters used for the simulation are gathered in Table 1.

The influence of C_0

As C_0 is increasing, mode-one killing is shifting into high position and high intensity according to Fig. 5. In order to fit with Imlay's experimental results C_0 has to stay in a range between 0.1 and 1 mM.

The influence of free available iron [Fe]

Iron chelators such as dipyridyl that can penetrate bacteria prevent external H_2O_2 from damaging DNA by reducing free available iron thanks to chelation (Imlay et al., 1988). Over-expression of ferritin, a storage protein that specifically sequesters iron also prevents damage (Keyer et al., 1995). But *E. coli* mutants that over-import iron are more sensitive to DNA damage when challenging external H_2O_2 (Touati et al., 1995). Fig. 6 reports the same conclusion with increasing damage when free available iron concentration increases.

3.3. Cell density involvement

Under conditions of exogenous H_2O_2 stress, H_2O_2 elimination is dependent on cell density. However, nothing is currently known about internal H_2O_2 concentration during H_2O_2 exposure. Under these conditions, internal H_2O_2 concentration results mostly from influx due to diffusion across the cell membrane, because endogenous production is negligible. Moreover, the more cell density increases, the faster the medium is detoxified. This phenomenon involves a decrease in exogenous H_2O_2 concentration and consequently in internal H_2O_2
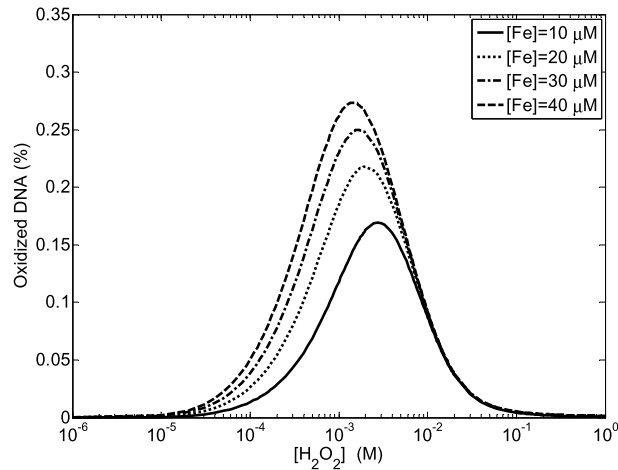
Figure 6. DNA oxidation (average during 15 minutes) dependence upon H_2O_2 external concentration and free available iron concentration. Parameter C_0 is set to 0.5 mM and v_{max} is set to $50\ \mu M\,s^{-1}$. Initially cell density was set to 10^7 cell/mL. The kinetic parameters used for the simulation are gathered in Table 1.
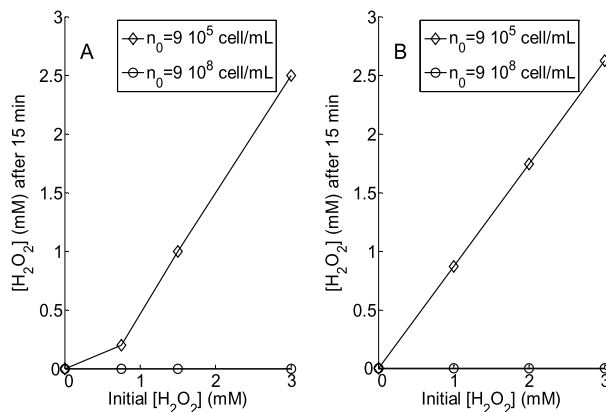
**Figure 7.** *E. coli* (MG1655) (*in vivo* A) cells were grown aerobically in liquid LB broth, at 37 °C, with shaking at 160 rpm. When the OD_{600} reached 1, the cells (diluted till 9×10^5/ml or not diluted) were exposed to various concentrations of H_2O_2 for 15 minutes. Extracellular H_2O_2 concentration was determined by TECAN readings at OD_{560}, with the Amplex® red hydrogen peroxide/peroxidase kit. Extracellular H_2O_2 concentration, determined after 15 minutes of incubation with various amounts of exogenous H_2O_2, in a wild-type strain incubated in LB, at 37 °C, in the presence of 400 ppm CO_2. Exogenous H_2O_2 concentration simulated under the same experimental conditions (*in silico* B).

concentration. Fig. 7 reports *in vivo* experimental detoxification of the medium with two different concentrations (A) and it also shows the corresponding *in silico* simulation which correctly fits the experiment (B).

As reported in Fig. 8, simulation shows that depending on cell density external average H_2O_2 concentration can be two orders of magnitude lower as the initial H_2O_2 exogenous concentration. This difference is involved in the disappearance of the mode one killing at high cell density as observed in Fig. 9.
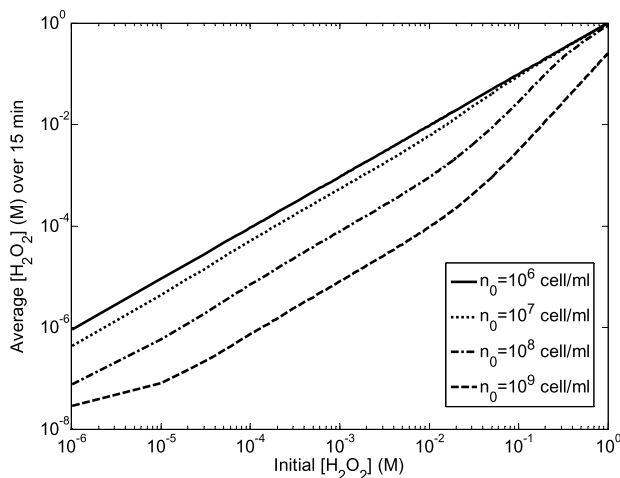
Figure 8. Simulation of the average H_2O_2 external concentration dependence with cell density and initial H_2O_2 exogenous concentration. The kinetic parameters used for the simulation are gathered in Table 1.
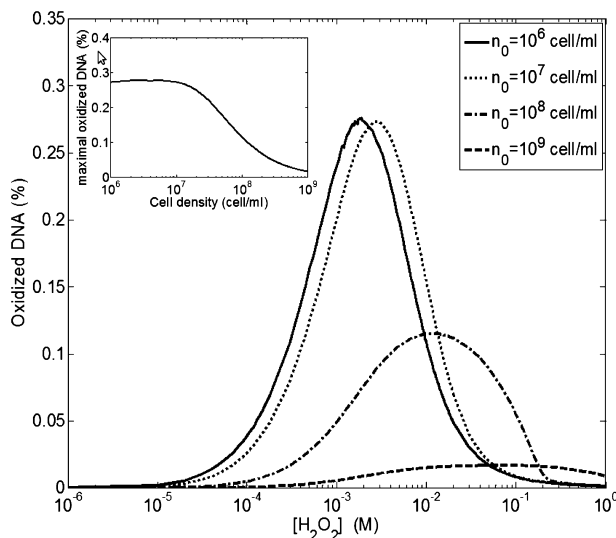
Figure 9. Simulation of the average oxidized DNA proportion dependence with cell density and initial H_2O_2 exogenous concentration. Inset shows the maximal oxidized DNA proportion dependence with cell density. The kinetic parameters used for the simulation are gathered in Table 1.

The major characteristics (intensity, width, position) of mode one killing is strongly dependent on cell density. Whereas the mode one killing seems to be present under 3×10^7 cell/ml, it disappears over 10^8 cell/ml. This phenomenon has been observed experimentally by our team (unpublished data). Indeed even at 10^8 cell/ml the mode one killing may disappear because it may be combined with mode two killing which emerges after 10 mM. This phenomenon is particularly non-linear (see inset of Fig. 9) whereas external average H_2O_2 concentration follows a nearly linear evolution compared with initial H_2O_2 exogenous or compared with cell density.

4. Conclusions

We present here a simple model that allows the understanding of DNA oxidation dynamics within *E. coli* after H$_2$O$_2$ exposure. The objective of the model presented is to essentially describe in a dynamic way the nature of H$_2$O$_2$ toxicity to an organism, in this case *E. coli*. Even if this model could seem imperfect, we believe that the scientific community will be able to challenge and improve it. For instance, using this approach, we were able to demonstrate iron or cell density involvement in HO$^\bullet$ dynamic and by consequence in DNA oxidation within *E. coli*. Indeed, without taking into account the evolution of those two parameters, we were not able to reproduce mode one killing experimental results obtained in the literature. Moreover the first killing mode can only be explained with iron decrease and not with quenching reactions which are responsible for slowing down oxidation but not for the oxidation peak.

> "Remember that all models are wrong; the practical question is how wrong do they have to be to not be useful."
>
> [— Box and Draper, Empirical Model-Building, p. 74.]

Declarations

Author declaration statement

Lionel Uhl, Sam Dukan: Conceived and designed the experiments; Analyzed and interpreted the data; Wrote the paper.

Audrey Gerstel, Maialène Chabalier: Performed the experiments.

Funding statement

Competing interest statement

The authors declare no conflict of interest.

Additional information

The following supplementary material is associated with this article:
Supplementary Material A, Supplementary Material B.

Acknowledgements

References

Antunes, F., Salvador, A., Marinho, H.S., Alves, R., Pinto, R.E., 1996. Lipid peroxidation in mitochondrial inner membranes. I. An integrative kinetic model. Free Radic. Biol. Med. 21, 917–943.

Aslund, F.M., Zheng, J., Beckwith Storz, G., 1999. Regulation of the OxyR transcriptional factor by hydrogen peroxide and the cellular thioldisulfide status. Proc. Natl. Acad. Sci. USA 96, 6161–6165.

Bennett, B.D., Kimball, E.H., Gao, M., Osterhout, R., Van Dien, S.J., Rabinowitz, J.D., 2009. Absolute metabolite concentrations and implied enzyme active site occupancy in Escherichia coli. Nat. Chem. Biol. 5, 593–599.

Bertrand, R.L., 2014. Lag phase-associated iron accumulation is likely a microbial counter-strategy to host iron sequestration: role of the ferric uptake regulator (fur). J. Theor. Biol. 21 (359), 72–79.

Brumaghim, J.L., Li, Y., Henle, E., Linn, S., 2003. Effects of hydrogen peroxide upon nicotinamide nucleotide metabolism in Escherichia coli: changes in enzyme levels and nicotinamide nucleotide pools and studies of the oxidation of NAD(P)H by Fe(III). J. Biol. Chem. 278, 42495–42504.

Buxton, G.V., Greenstock, C.L., 1988. Critical review of rate constants for reactions of hydrated electrons. J. Phys. Chem. Ref. Data 17, 513886.

Fridovich, I., 1978. The biology of oxygen radicals. Science 201, 875–880.

Giannessi, M., Del Corso, A., Cappiello, M., Voltarelli, M., Marini, I., Barsacchi, D., Garland, D., Camici, M., Mura, U., 1993. Thiol-dependent metal-catalyzed oxidation of bovine lens aldose reductase. I. Studies on the modification process. Arch. Biochem. Biophys. 300, 423–429.

Gonzalez-Flecha, B., Demple, B., 1995. Metabolic sources of hydrogen peroxide in aerobically growing Escherichia coli. J. Biol. Chem. 270, 13681–13687.

Hallin, P.F., Ussery, D.W., 2004. CBS Genome Atlas Database: a dynamic storage for bioinformatic results and sequence data. Bioinformatics 20, 3682–3686.

Hillar, A., Peters, B., Pauls, R., Loboda, A., Zhang, H., Mauk, A.G., Loewen, P.C., 2000. Modulation of the activities of catalase-peroxidase HPI of Escherichia coli by site-directed mutagenesis. Biochemistry 59, 5868–5875.

Hsieh, Y.H., Hsieh, Y.P., 2000. Kinetics of Fe(III) reduction by ascorbic acid in aqueous solutions. J. Agric. Food Chem. 48, 1569–1573.

Imlay, J.A., 2003. Pathways of oxidative damage. Annu. Rev. Microbiol. 57, 395–418.

Imlay, J.A., 2013. The molecular mechanisms and physiological consequences of oxidative stress: lessons from a model bacterium. Nat. Rev. Microbiol. 11, 443–454.

Imlay, J.A., Chin, S.M., Linn, S., 1988. Toxic DNA damage by hydrogen peroxide through the Fenton reaction in vivo and in vitro. Science 240, 640–642.

Imlay, J.A., Fridovich, I., 1991. Assay of metabolic superoxide production in Escherichia coli. J. Biol. Chem. 266, 6957–6965.

Imlay, J.A., Linn, S., 1986. Bimodal pattern of killing of DNA-repair-defective or anoxically grown Escherichia coli by hydrogen peroxide. J. Bacteriol. 166, 519–527.

Imlay, J.A., Linn, S., 1988. DNA damage and oxygen radical toxicity. Science 240, 1302–1309.

Jimenez-Del-Rio, M., Velez-Pardo, C., 2012. The bad, the good and the ugly about oxidative stress. Oxid. Med. Cell. Longev., 163913.

Keyer, K., Gort, A.S., Imlay, J.A., 1995. Superoxide and the production of oxidative DNA damage. J. Bacteriol. 177, 6782–6790.

Keyer, K., Imlay, J.A., 1996. Superoxide accelerates DNA damage by elevating free-iron levels. Proc. Natl. Acad. Sci. USA 93, 13635–13640.

Koppenol, W.H., 2001. The Haber–Weiss cycle – 70 years later. Redox Rep. 6, 229–234.

Kowald, A., Lehrach, H., Klipp, E., 2006. Alternative pathways as mechanism for the negative effects associated with overexpression of superoxide dismutase. J. Theor. Biol. 238, 828–840.

Liochev, S.I., Fridovich, I., 2002. The Haber–Weiss cycle – 70 years later: an alternative view. Redox Rep. 7, 59–60.

Luo, Y., Han, Z., Chin, S.M., Linn, S., 1994. Three chemically distinct types of oxidants formed by iron-mediated Fenton reactions in the presence of DNA. Proc. Natl. Acad. Sci. USA 91, 12438–12442.

Macomber, L., Rensing, C., Imlay, J.A., 2007. Intracellular copper does not catalyze the formation of oxidative DNA damage in Escherichia coli. J. Bacteriol. 189, 1616–1626.

Michaels, H.B., Hunt, J.W., 1973. Reactions of the hydroxyl radical with polynucleotides. Radiat. Res. 56, 57–70.

Netto, L.E., Stadtman, E.R., 1996. The iron-catalyzed oxidation of dithiothreitol is a biphasic process: hydrogen peroxide is involved in the initiation of a free radical chain of reactions. Arch. Biochem. Biophys. 333, 233–242.

Park, S., You, X., Imlay, J.A., 2005. Substantial DNA damage from submicromolar intracellular hydrogen peroxide detected in Hpx-mutants of Escherichia coli. Proc. Natl. Acad. Sci. USA 102, 9317–9322.

Polynikis, A., Hogan, S.J., di Bernardo, M., 2009. Comparing different ODE modelling approaches for gene regulatory networks. J. Theor. Biol. 261, 511–530.

Seaver, L.C., Imlay, J.A., 2001a. Alkyl hydroperoxide reductase is the primary scavenger of endogenous hydrogen peroxide in Escherichia coli. J. Bacteriol. 183 (24), 7173–7181.

Seaver, L.C., Imlay, J.A., 2001b. Hydrogen peroxide fluxes and compartmentalization inside growing Escherichia coli. J. Bacteriol. 183 (24), 7182–7189.

Seaver, L.C., Imlay, J.A., 2004. Are respiratory enzymes the primary sources of intracellular hydrogen peroxide? J. Biol. Chem. 279, 48742–48750.

Touati, D., Jacques, M., Tardat, B., Bouchard, L., Despied, S., 1995. Lethal oxidative damage and mutagenesis are generated by iron in delta fur mutants of Escherichia coli: protective role of superoxide dismutase. J. Bacteriol. 177, 2305–2314.

Valko, M., Morris, H., Cronin, M.T.D., 2005. Metals, toxicity and oxidative stress. Curr. Med. Chem. 12, 1161–1208.